Int. J. Solids Structures Vol. 30, No. 2, pp. 177–198, 1993
Printed in Great Britain.

0020–7683/93 $5.00+ .00

A MICROCRACK DAMAGE MODEL FOR BRITTLE MATERIALS

LUIGI GAMBAROTTA and SERGIO LAGOMARSINO
Istituto di Scienza delle Costruzioni, Università di Genova,
Via Montallegro, 1—16145 Genova, Italy

(*Received* 29 *February* 1992; *in revised form* 16 *June* 1992)

Abstract—A damage model for brittle materials subject to arbitrary stress is developed. By considering dilute distributions of flat microcracks, self-similarly propagating in a linear elastic matrix, constitutive equations are obtained taking into account both stress- and damage-induced anisotropy. The crack size and, for closed cracks, the frictional sliding vector are assumed as internal variables; the evolution equations, obtained through properly defined sliding and crack growth criteria, make it possible to state the limit conditions of the stable response to applied stresses. Comparisons between experimental and theoretical results related to different loading paths show the capabilities of the model. Finally the unstable response to uniaxial stresses is analysed in order to show the influence of the stressing mode and of the crack distribution on the post-peak behavior.

1. INTRODUCTION

It is well known that brittle and quasi-brittle materials (e.g. ceramics, mortar, concrete, rocks and brittle composite materials) exhibit, in loading processes, a progressive loss of stiffness (up to a limit load beyond which strain softening takes place), stress-induced anisotropy, dilatancy and linearity in the unloading phase with vanishing residual strains. Such mechanical behavior is commonly attributed to the presence of material defects, like flaws and voids. In a loading process, existing defects may grow and coalesce and new defects may be nucleated inducing a progressive change in the material microstructure, the damage, to which the loss of stiffness is directly related.

Several continuum phenomenological and micromechanical damage models have been proposed [see for reference, Krajcinovic (1989)], in which the changes in the material structure are generally described through the evolution of suitably defined internal variables. Although phenomenological models have been proposed in order to account for the anisotropic stiffness degradation due to the different behavior of the defects under compressive or tensile stress, an effective description of the anisotropic damage in brittle and quasi-brittle materials can be obtained through a micromechanical approach, based on the model of an elastic solid containing growing microcracks.

In modeling a given material as a microcrack-weakened elastic solid it is necessary, at first, to assume suitable hypotheses on the crack geometry and distribution inside the representative volume element; then, in order to develop the constitutive equations by means of homogenization techniques, the microcrack response to applied stresses must be formulated with reference both to the displacement jumps across the crack faces, that contribute to the macrostrain, and to the kinetics of the crack growth that characterizes the damage process. The effect of the frictional contact between the crack faces, which markedly affects the model response, can easily be taken into account if moderate microcrack concentrations are assumed; in this case the hypothesis of ignoring the disturbance in the stress field due to the presence of the other microcracks allows simple relations between the contact tractions and the macrostresses to be resolved on the crack plane.

The model by Krajcinovic and Fanella (1986), proposed in order to simulate the damage in concrete under tensile stresses, is developed by assuming self-similar propagating circular flat cracks; the displacement discontinuities across the crack faces are evaluated neglecting the crack interaction effects. Since in macroscopically isotropic brittle materials, at rupture inception, the propagation of the closed microcracks may be not self-similar, in the models by Kachanov (1982a, b), Nemat-Nasser and Obata (1988) and Fanella and Krajcinovic (1988) the kinetics of the crack growth have been described by considering

straight and kinked cracks, the latter being modeled by means of an equivalent two-dimensional crack system; moreover in these models the crack interaction effects have been neglected. The two-dimensional model by Sumarac and Krajcinovic (1987, 1989) and Krajcinovic and Sumarac (1989) takes into account the crack interaction effect on the compliance of the microcrack-weakened elastic solid through the self-consistent method applied to a two-dimensional distribution of growing straight cracks; however, from the analysis developed by the authors, related to uniaxial tensile stress, it is emphasized that good accuracy may be obtained even with the assumption of non-interacting cracks. Recently, Ju (1991) formulated a two-dimensional model which takes into account both the self-similar propagation and the kinking of straight cracks; kinked cracks are modeled through an equivalent straight crack and the interaction effect is taken into account through the self-consistent method.

In this paper a damage model for brittle materials, based on the hypothesis of self-similar growth of non-interacting flat cracks is developed. It is pointed out that the model, which is rigorously valid only for special cases (e.g. dilute crack concentrations, interface cracks, etc.), may give acceptable results for initially isotropic materials up to rupture inception. Moreover the model is also effective when non-proportional loading paths, eventually inducing triaxial stress states, are considered; in this case the two-dimensional kinked crack models may be employed, but with difficulty, and the self-consistent method, which markedly underestimates the overall stiffness of the microcracked model (Hashin, 1988) is cumbersome to apply.

The microcrack ensemble is described through orientations, each related to a set of equioriented cracks; to each orientation is associated the crack size and, for closed cracks, the frictional sliding vector, which are considered as internal variables. Through properly defined sliding and crack growth criteria, the evolution equations giving the rate of the internal variables are obtained, which allow the formulation of the incremental constitutive equations and the stating of the limit conditions for the model, whose response becomes unstable once such conditions are attained. A finite step numerical procedure for evaluating the strain increments corresponding to given stress increments is developed and employed to analyse the model response under non-proportional loadings. The examples point out the effect of stress- and damage-induced anisotropy; some comparisons between the theoretical and experimental results related to different loading paths show the good capabilities of the proposed model together with its validity limits. Finally the unstable response to uniaxial stresses is analysed from which it emerges that the stressing mode and the assumed microcrack distribution affect the post-peak behavior, that may exhibit snap-back instability.

2. THE MICROCRACKED ELASTIC SOLID

The material is modeled as a solid constituted by a linear isotropic elastic matrix containing plane microcracks, growing in the loading process. In order to obtain constitutive equations for the considered solid under consideration, reference is made to the macrostress $\mathbf{T}$ and macrostrain $\mathbf{E}$ (Nemat-Nasser and Horii, 1990); the latter is given as the sum of the mean strain in the matrix and of the contribution of the discontinuities in the displacement field due to the presence of the microcracks:

$$\mathbf{E} = \mathbb{K}\mathbf{T} + \frac{1}{V}\sum \int_{\mathscr{A}_c} \operatorname{sym}\left[\mathbf{u}^*(\boldsymbol{\xi}) \otimes \mathbf{n}\right] \mathrm{d}A, \tag{1}$$

where $\mathbb{K}$ is the compliance fourth-order tensor of the elastic matrix, the sum involves all the cracks inside the representative volume element $\mathscr{V}$ (of measure V), $\mathscr{A}_c$ is the surface of a crack having normal $\mathbf{n}$ to the crack plane, and $\mathbf{u}^*(\boldsymbol{\xi})$ is the displacement jump between the opposite faces of the crack at a point whose location is given by the vector $\boldsymbol{\xi}$ in the local crack reference.

The ensemble of cracks inside the representative unit volume is represented by $\mathcal{N}$ subsets; the ith subset is composed of n_i equioriented cracks and is identified by the unit vector $\mathbf{n}_i$ normal to their crack planes. Moreover these cracks have the same shape and equal characteristic size a_i; their orientation in the plane of normal $\mathbf{n}_i$, defined by the unit vector $\mathbf{m}$, is random. Since the crack growth is assumed to be self-similar, in the loading process all the cracks of a subset are characterized only by their size. Following this approach the $\mathcal{N}$ subsets become a characteristic of the solid, since they state its symmetry group; for $\mathcal{N} \to \infty$, when a and n are equal for each subset, the solid tends to be isotropic.

The contribution to the strain due to the microcracks can be expressed as follows:

$$\mathbf{E}_c = \sum_{i=1}^{\mathcal{N}} \sum_{j=1}^{n_i} \int_{\mathcal{A}_{cij}} [u_{ij}^*(\boldsymbol{\xi})\mathbf{n}_i \otimes \mathbf{n}_i + \mathrm{sym}\,[\mathbf{w}_{ij}^*(\boldsymbol{\xi}) \otimes \mathbf{n}_i]]\,\mathrm{d}A, \tag{2}$$

where u_{ij}^* and $\mathbf{w}_{ij}^*$ are the jump displacements, respectively normal and tangential to the crack.

If the crack interaction is neglected and the crack faces are assumed to be traction free, from the reciprocity theorem applied to a single flat crack inside an infinite elastic solid, it follows that the jump displacement across the faces of the crack of normal $\mathbf{n}_i$ depends on the resolved stresses on the crack plane $\sigma_i = \mathbf{n}_i \cdot \mathbf{T}\mathbf{n}_i$, $\boldsymbol{\tau}_i = (\mathbf{I} - \mathbf{n}_i \otimes \mathbf{n}_i)\mathbf{T}\mathbf{n}_i$, as follows:

$$u_{ij}^*(\boldsymbol{\xi}) = g_i(E, \nu, a_i, \boldsymbol{\xi})\sigma_i, \tag{3a}$$

$$\mathbf{w}_{ij}^*(\boldsymbol{\xi}) = \mathbf{R}_i(\mathbf{m}_j)\mathbf{G}_i(E, \nu, a_i, \boldsymbol{\xi})\mathbf{R}_i(\mathbf{m}_j)^{\mathrm{T}}\boldsymbol{\tau}_i. \tag{3b}$$

Here g_i represents the characteristic function of the normal jump displacement, which depends on the crack size and shape, the elastic moduli E and ν of the matrix and on the location $\boldsymbol{\xi}$, and the tensorial function $\mathbf{G}_i$, expressed in the crack local reference, characterizes the tangential jump displacement, $\mathbf{R}_i(\mathbf{m}_j)$ being the rotation between the unit vector $\mathbf{m}_j$ and a reference vector.

By substituting eqns (3) in (2), because of the hypothesis of in-plane random crack orientation, it follows that

$$\mathbf{E}_c = \sum_{i=1}^{\mathcal{N}} n_i[g_i'\sigma_i\mathbf{n}_i \otimes \mathbf{n}_i + \mathrm{sym}\,(g_i''\boldsymbol{\tau}_i \otimes \mathbf{n}_i)], \tag{4}$$

where g_i' and g_i'' are scalar functions, related to the crack shape.

Equation (4) implies that each subset of microcracks contributes to the macrostrain through an extension and a slide respectively given by

$$\varepsilon_i = n_i g_i'(E, \nu, a_i)\sigma_i, \tag{5a}$$

$$\gamma_i = n_i g_i''(E, \nu, a_i)\tau_i, \tag{5b}$$

the latter showing an isotropic dependence of the sliding on the shearing stress. By means of a dimensional analysis of eqns (5) it follows that

$$\varepsilon_i = c_{ni}\alpha_i^3\sigma_i, \tag{6a}$$

$$\gamma_i = c_{ti}\alpha_i^3\tau_i, \tag{6b}$$

where $\alpha_i = a_i/a_{0i}$ is the ratio between the actual crack size and the reference one and the constants c_{ni} and c_{ti} represent, respectively, the extensional and sliding compliance of the ith subset when no crack grows:

$$c_{ni} = \frac{n_i a_{0i}^3}{E} \bar{g}_i(\nu), \tag{7a}$$

$$c_{ti} = \frac{n_i a_{0i}^3}{E} \bar{\bar{g}}_i(\nu). \tag{7b}$$

Equations (6) hold even though different sets of randomly distributed parallel cracks are considered, each one having a different shape but the same size; in this case the constants c_{ni} and c_{ti} can be obtained through a superposition of the compliances related to each set, whose form is analogous to that given in eqns (7). Instead of evaluating the above-mentioned constants on the basis of the crack shape, it seems more appropriate to consider them as model parameters, to be determined by experiments; so the parameters characterizing the microcracked elastic solid are the elastic moduli of the matrix, the orientations $\mathbf{n}_i$ of the $\mathcal{N}$ subsets and the related compliances c_{ni} and c_{ti}.

The equations obtained, related to the traction-free condition on the crack faces, may be extended to include the effect of the contact tractions acting on the opposite faces of closed cracks. To this end the assumption is made that uniform self-equilibrated tractions, respectively having normal $p_i\mathbf{n}_i$ and tangential $\mathbf{f}_i$ components, act on the crack faces of normal $\mathbf{n}_i$. This approach, which is rigorous for penny-shaped cracks, allows a simple description of the effects of the contact tractions by rewriting eqns (6) in the following forms:

$$\varepsilon_i = c_{ni}\alpha_i^3(\sigma_i - p_i), \tag{8a}$$

$$\gamma_i = c_{ti}\alpha_i^3(\tau_i - \mathbf{f}_i). \tag{8b}$$

Once the macrostress $\mathbf{T}$ and the variables p_i, $\mathbf{f}_i$ and α_i for each orientation $\mathbf{n}_i$ are known, and thus, by eqn (8), the corresponding extension ε_i and slide γ_i, the macrostrain $\mathbf{E}$ is obtained:

$$\mathbf{E} = \mathbb{K}\mathbf{T} + \sum_{i=1}^{\mathcal{N}} [\varepsilon_i \mathbf{n}_i \otimes \mathbf{n}_i + \mathrm{sym}\,(\gamma_i \otimes \mathbf{n}_i)]. \tag{9}$$

Since the dependence of the variables p_i, $\mathbf{f}_i$ and α_i on the macrostress $\mathbf{T}$ is given by anholonomic relations, as will be shown in later sections, constitutive equations (9) must be expressed in incremental form. So the extension and the slide rates related to the ith plane are given by:

$$\dot{\varepsilon}_i = c_{ni}\alpha_i^2[(\dot{\sigma}_i - \dot{p}_i)\alpha_i + 3(\sigma_i - p_i)\dot{\alpha}_i], \tag{10a}$$

$$\dot{\gamma}_i = c_{ti}\alpha_i^2[(\dot{\tau}_i - \dot{\mathbf{f}}_i)\alpha_i + 3(\tau_i - \mathbf{f}_i)\dot{\alpha}_i], \tag{10b}$$

showing two different effects: the former due to the resolved stress rate and to the contact tractions rate, the latter due to the crack growth rate. Equations (10) are meaningful once the evolution laws of the contact variables p_i, $\mathbf{f}_i$ and of the damage variable α_i are expressed in terms of the macrostress rate $\dot{\mathbf{T}}$.

At a generic state of the loading process the specific dissipation rate D is given by

$$D = \sum_{i=1}^{\mathcal{N}} (p_i\dot{\varepsilon}_i + \mathbf{f}_i \cdot \dot{\gamma}_i + \mathscr{G}_i\dot{\alpha}_i), \tag{11}$$

where $\mathscr{G}_i$ is the strain energy release related to all the cracks of normal $\mathbf{n}_i$, defined as

$$\mathscr{G}_i = \tfrac{3}{2}\alpha_i^2[c_{ni}(\sigma_i - p_i)^2 + c_{ti}(\tau_i - \mathbf{f}_i)\cdot(\tau_i - \mathbf{f}_i)]. \tag{12}$$

The specific dissipation rate related to the ith orientation is due to both the dissipative work

of the contact tractions on the corresponding deformations rate and the strain energy release due to the crack growth rate.

From eqns (11), (8) and (12), it turns out that ε_i, γ_i and α_i may be assumed to be internal variables of the model to which are associated, respectively, p_i, $\mathbf{f}_i$, $\mathscr{G}_i$ $(i = 1, \mathscr{N})$.

3. SLIDING AND CRACK GROWTH CRITERIA

In the loading process the internal variables and the resolved stresses on the crack planes of normal $\mathbf{n}$ (in Sections 3 and 4 the index i will be omitted) are subjected to two conditions concerning both the friction contact between the crack faces and the crack growth.

As regards the friction contact in closed cracks, the hypothesis that the tractions p (<0) and $\mathbf{f}$ must satisfy the Coulomb condition is assumed, that is

$$\phi_s = |\mathbf{f}| + \mu p \leqslant 0, \tag{13}$$

where μ is the friction coefficient, to be considered as a further model parameter. If in an infinitesimal step the conditions $\phi_s = \dot{\phi}_s = 0$ are attained, then it is assumed that a slide takes place in the direction of the unit vector $\mathbf{v} = \mathbf{f}/|\mathbf{f}|$, with no extension:

$$\dot{\varepsilon} = 0, \tag{14a}$$

$$\dot{\gamma} = \mathbf{v}\dot{\lambda}, \quad \dot{\lambda} \geqslant 0. \tag{14b}$$

The traction p may be obtained as a function of the normal stress σ so that the extension ε and the traction p need not be considered as internal variables of the model. Since for closed cracks no extension is allowed, the unilateral contact conditions are

$$\varepsilon \geqslant 0, \tag{15a}$$

$$p \leqslant 0, \tag{15b}$$

$$p\varepsilon = 0, \tag{15c}$$

these conditions, together with eqn (8a), lead to

$$\sigma < 0, \quad p = \sigma, \tag{16a}$$

$$\sigma \geqslant 0, \quad p = 0, \tag{16b}$$

from which it follows that if $\sigma \geqslant 0$ no contact traction is effective (open cracks). It is worthwhile noting, as will be shown in Section 4, that the sliding rule (14b) does not allow crack growth when no sliding occurs.

The second condition concerns the crack growth $(\dot{\alpha} > 0)$, ruled by a fracture propagation criterion. The hypothesis is advanced that the propagation of the $\mathbf{n}$-oriented cracks may take place when the strain energy release $\mathscr{G}$ equals the resistance to crack growth $\mathscr{R}$. On the contrary, if $\mathscr{G} < \mathscr{R}$ no propagation takes place $(\dot{\alpha} = 0)$. So the resistance $\mathscr{R}$ is assumed to be the overall measure of the fracture toughness related to the $\mathbf{n}$-oriented microcracks. It follows that the admissible states must satisfy the following conditions:

$$\phi_d = \mathscr{G} - \mathscr{R} \leqslant 0. \tag{17}$$

In an infinitesimal step, if the conditions $\phi_d = \dot{\phi}_d = 0$ are attained, then a crack growth $(\dot{\alpha} > 0)$ is postulated.

Likewise the fracture criteria based on the resistance curve [see for reference Broek (1986) and Ouyang *et al.* (1990)] and with the aim of modeling both stable and unstable crack growth, the resistance to crack growth $\mathscr{R}$ is assumed as a positive growing function

of the damage variables α in the range $[1, +\infty)$. The limiting case in which fracture toughness is assumed to be a constant corresponds to the Griffith criterion.

4. DAMAGE AND SLIDING EVOLUTION EQUATIONS

The above sliding and crack growth criteria allow us to formulate the damage and sliding evolution equations (the latter is meaningful only for closed cracks), giving $\dot{\alpha}$ and $\dot{\gamma}$ as functions of the resolved stress rates $\dot{\sigma}$ and $\dot{\tau}$. These equations vary according to whether microcracks are open or closed.

(a) *Open microcracks* ($\sigma \geqslant 0$)

Since contact tractions are vanishing ($p = 0$, $\mathbf{f} = \mathbf{0}$), the extension and slide depend only on the resolved stresses, so condition (17) becomes:

$$\Phi_d^+ = \tfrac{3}{2}\alpha^2[c_n\sigma^2 + c_t\boldsymbol{\tau}\cdot\boldsymbol{\tau}] - \mathscr{R}(\alpha) \leqslant 0. \tag{18}$$

Crack growth is only possible if $\Phi_d^+ = 0$ and the damage rate $\dot{\alpha}$ is obtained as the solution of the following linear complementarity problem:

$$\dot{\Phi}_d^+ = 3\alpha^2(c_n\sigma\dot{\sigma} + c_t\boldsymbol{\tau}\cdot\dot{\boldsymbol{\tau}}) - \mathscr{D}\dot{\alpha} \leqslant 0, \tag{19a}$$

$$\dot{\alpha} \geqslant 0, \tag{19b}$$

$$\dot{\Phi}_d^+\dot{\alpha} = 0, \tag{19c}$$

having defined

$$\mathscr{D} = \frac{\partial(\mathscr{R} - \mathscr{G})}{\partial\alpha} = \mathscr{R}'(\alpha) - 3\alpha(c_n\sigma^2 + c_t\boldsymbol{\tau}\cdot\boldsymbol{\tau}). \tag{20}$$

The solution to this problem essentially depends on the sign of $\mathscr{D}$ and on the stress rates $\dot{\sigma}$ and $\dot{\boldsymbol{\tau}}$ through the scalar variable

$$s = \sigma\dot{\sigma} + \rho\boldsymbol{\tau}\cdot\dot{\boldsymbol{\tau}}, \tag{21}$$

being $\rho = c_t/c_n$, and is given as follows:

$$\mathscr{D} > 0, \quad s \leqslant 0, \quad \dot{\alpha} = 0, \tag{22a}$$

$$s > 0, \quad \dot{\alpha}3c_n\alpha^2 s/\mathscr{D}; \tag{22b}$$

$$\mathscr{D} = 0, \quad s < 0, \quad \dot{\alpha} = 0, \tag{22c}$$

$$s = 0, \quad \dot{\alpha} \geqslant 0 \quad \text{(undetermined)}, \tag{22d}$$

$$s > 0, \quad \text{no solution};$$

$$\mathscr{D} < 0, \quad s \leqslant 0, (1) \quad \dot{\alpha} = 0, \tag{22e}$$

$$(2) \quad \dot{\alpha} = 3c_n\alpha^2 s/\mathscr{D}, \tag{22f}$$

$$s > 0, \quad \text{no solution.}$$

It is worth noting that no solution exists if $\mathscr{D} \leqslant 0$ and $s > 0$, while if $s \leqslant 0$ two solutions are given, which are associated with different values of the extension and slide rates [see eqns (10)].

At the initial phase of a loading process, considering that from eqn (20) for vanishing stresses $\mathscr{D} > 0$ follows, a stable crack growth takes place. A limit state is identified when the condition $\mathscr{D} = 0$ is attained, since further stress increments must obey the condition of non-positiveness of the variable s; the possibility that the above condition may be satisfied

also depends on the choice of the toughness function $\mathscr{R}(\cdot)$. By considering eqns (18) and (20), the value α_c of the damage variable at the limit state is the solution of the following equation:

$$\mathscr{R}'(\alpha_c) - 2\mathscr{R}(\alpha_c)/\alpha_c = 0, \tag{23}$$

and is characteristic of the chosen toughness function. Once the limit state is attained, two different paths may be followed: in the former, cracks are stable ($\dot{\alpha} = 0$), while in the latter cracks are unstable ($\dot{\alpha} > 0$).

(b) *Closed microcracks* ($\sigma < 0$)

Since in this case contact tractions on the crack faces are active, both the sliding and the crack growth criteria must be satisfied.

The sliding criterion may be expressed, through equations (8b), (13) and (16), as a function of the resolved stresses and of the internal variables γ and α:

$$\Phi_s = |\tau - \gamma/c_t\alpha^3| + \mu\sigma \leqslant 0. \tag{24}$$

When $\Phi_s = 0$, the rates $\dot{\alpha}$ and $\dot{\lambda}$ must satisfy the conditions:

$$\dot{\Phi}_s = -\frac{1}{c_t\alpha^3}\dot{\lambda} + \frac{3}{c_t\alpha^4}\mathbf{v}\cdot\gamma\dot{\alpha} + \mathbf{v}\cdot\dot{\tau} + \mu\dot{\sigma} \leqslant 0, \tag{25a}$$

$$\dot{\lambda} \geqslant 0, \quad \dot{\alpha} \geqslant 0, \tag{25b}$$

$$\dot{\Phi}_s\dot{\lambda} = 0, \tag{25c}$$

where the unit vector $\mathbf{v}$ depends, through eqn (8b), on the tangential stress τ and on the variables γ and α.

Vice versa, the crack growth criterion (17) can be expressed, with $p = \sigma$ and through eqns (8) and (12), in terms of the internal variables α and γ alone:

$$\Phi_d^- = \frac{3}{2c_t\alpha^4}\gamma\cdot\gamma - \mathscr{R}(\alpha) \leqslant 0. \tag{26}$$

When $\Phi_d^- = 0$, the rates $\dot{\alpha}$ and $\dot{\lambda}$ must satisfy the conditions:

$$\dot{\Phi}_d^- = \frac{3}{c_t\alpha^4}\mathbf{v}\cdot\gamma\dot{\lambda} - \left[\frac{6}{c_t\alpha^5}\gamma\cdot\gamma + \mathscr{R}'\right]\dot{\alpha} \leqslant 0, \tag{27a}$$

$$\dot{\lambda} \geqslant 0, \quad \dot{\alpha} \geqslant 0, \tag{27b}$$

$$\dot{\Phi}_d^-\dot{\alpha} = 0. \tag{27c}$$

It turns out that, for evaluating the rates $\dot{\alpha}$ and $\dot{\lambda}$, four different cases are possible.

The case in which $\Phi_s < 0$, $\Phi_d^- < 0$ obviously involves no sliding or crack growth ($\dot{\lambda} = 0$, $\dot{\alpha} = 0$). The same result is obtained when $\Phi_s < 0$, $\Phi_d^- = 0$, since, from eqn (27), the absence of sliding ($\dot{\lambda} = 0$) implies no crack growth ($\dot{\alpha} = 0$); this follows from the sliding rule (14b) which implicitly establishes a dependence of the damage variable on the sliding.

On the contrary, sliding may take place without attaining the crack growth criterion ($\Phi_s = 0$, $\Phi_d^- < 0$); having defined the scalar

$$\ell = \mu\dot{\sigma} + \mathbf{v}\cdot\dot{\tau}, \tag{28}$$

the slide rate is found to be the solution of the linear complementarity problem (25), in which $\dot{\alpha} = 0$ is put,

$$\ell \leqslant 0, \quad \dot{\lambda} = 0, \tag{29a}$$

$$\ell > 0, \quad \dot{\lambda} = c_t \alpha^3 \ell. \tag{29b}$$

Finally, when $\Phi_s = \Phi_d^- = 0$, the rates $\dot{\alpha}$ and $\dot{\lambda}$ are obtained as the solutions of the linear complementarity problem (25)–(27), which admits a unique solution if and only if the matrix

$$\mathbf{A} = \begin{bmatrix} \dfrac{1}{c_t \alpha^3} & -\dfrac{3}{c_t \alpha^4} \mathbf{v} \cdot \boldsymbol{\gamma} \\ -\dfrac{3}{c_t \alpha^4} \mathbf{v} \cdot \boldsymbol{\gamma} & \dfrac{6}{c_t \alpha^5} \boldsymbol{\gamma} \cdot \boldsymbol{\gamma} + \mathscr{R}' \end{bmatrix}, \tag{30}$$

is positive definite. From the above assumption it follows that $\mathbf{A}$ is positive definite if

$$\det \mathbf{A} = \frac{1}{c_t \alpha^3} \left[\mathscr{R}' - \frac{3}{c_t \alpha^5} |\boldsymbol{\gamma}|^2 (1 - 3 \sin^2 \varphi) \right] > 0, \tag{31}$$

where φ is the angle between the unit vector $\mathbf{v}$ and the sliding vector $\boldsymbol{\gamma}$. It turns out that the solution depends on the sign of $\det \mathbf{A}$:

$\det \mathbf{A} > 0$

$$\ell \leqslant 0, \qquad \dot{\lambda} = 0, \quad \dot{\alpha} = 0, \tag{32a}$$

$$\ell > 0 \quad \text{(a)} \ \cos \varphi \leqslant 0, \quad \dot{\lambda} = c_t \alpha^3 \ell, \quad \dot{\alpha} = 0, \tag{32b}$$

$$\text{(b)} \ \cos \varphi > 0, \quad \dot{\lambda} = \ell \left[\frac{6|\boldsymbol{\gamma}|^2}{c_t \alpha^5} + \mathscr{R}' \right] \Big/ \det \mathbf{A}, \quad \dot{\alpha} = \ell \frac{3|\boldsymbol{\gamma}|}{c_t \alpha^4} \cos \varphi / \det \mathbf{A}; \tag{32c}$$

$\det \mathbf{A} = 0$

$$\ell < 0, \qquad \dot{\lambda} = 0, \quad \dot{\alpha} = 0, \tag{32d}$$

$$\ell = 0 \quad \text{(a)} \ \dot{\lambda} = 0, \quad \dot{\alpha} = 0, \tag{32e}$$

$$\text{(b)} \ \dot{\lambda} > 0 \ \text{ indeterminate}, \quad \dot{\alpha} = \frac{\alpha}{3|\boldsymbol{\gamma}| \cos \varphi} \dot{\lambda}, \tag{32f}$$

$$\ell > 0, \qquad \text{no solution;}$$

$\det \mathbf{A} < 0$

$$\ell \leqslant 0 \quad \text{(a)} \ \dot{\lambda} = 0, \quad \dot{\alpha} = 0, \tag{32g}$$

$$\text{(b)} \ \dot{\lambda} = \ell \left[\frac{6|\boldsymbol{\gamma}|^2}{c_t \alpha^5} + \mathscr{R}' \right] \Big/ \det \mathbf{A}, \quad \dot{\alpha} = t \frac{3|\boldsymbol{\gamma}|}{c_t \alpha^4} \cos \varphi / \det \mathbf{A}, \tag{32h}$$

$$\ell > 0, \qquad \text{no solution.}$$

The solutions (32a, d, e, g) imply no sliding, while the solution (32b) takes into account sliding with no crack growth; finally the solutions (32c, f, h) consider both sliding and

damage. A picture of the above solutions is shown in Fig. 1, where the rates of the stresses and of the internal variables are shown in the plane of the tangential stresses (for simplicity $\dot{\sigma} = 0$ is considered). In such a plane the tangential stress τ, the friction $\mathbf{f}$ and the vector $\gamma/c_t\alpha^3$, representative of the sliding, are shown; the no sliding domain (24) is a circle, having radius $|\mathbf{f}|$ and center at the end of the vector $\gamma/c_t\alpha^3$, whose motion in the stress plane is related to the sliding (the initial and the final state in the loading step are respectively represented by continuous and dashed lines).

When $\det \mathbf{A} > 0$, two different possibilities can be envisaged according to whether or not the stress rate involves the return of the stress point to within the no sliding domain. The first case [$\ell < 0$ (32a)], shown in Fig. 1(a), concerns stress rates which move the stress point inside the no sliding domain; the final state is $\Phi_s < 0$, $\Phi_d^- = 0$. This case is also representative of the solution (29a). In the second case ($\ell > 0$) two further possibilities must be distinguished from the value of the angle φ, between $\mathbf{f}$ and γ. For $|\varphi| > \pi/2$ [see eqn (32b) and Fig. 1(b)] $\dot{\gamma}$ involves a decrease in $|\gamma|$ and, since $\alpha \geqslant 1$, the consequence is $\dot{\Phi}_d^- < 0$; the no sliding domain moves in the direction of $\mathbf{f}$ and it follows that at the end of the step $\Phi_s = 0$, $\Phi_d^- < 0$. This case is also representative of the solution (29b). On the contrary, for $|\varphi| < \pi/2$ [see eqn (32c) and Fig. 1(c)] $\dot{\gamma}$ increases $|\gamma|$ and then, in order to satisfy condition (26), $\dot{\alpha} > 0$ must be attained; by virtue of eqn (10b), it follows that the motion of the no sliding domain is given by the vector $(\dot{\gamma} - 3\gamma\dot{\alpha}/\alpha)/c_t\alpha^3$ and the final state is $\Phi_s = 0$, $\Phi_d^- = 0$.

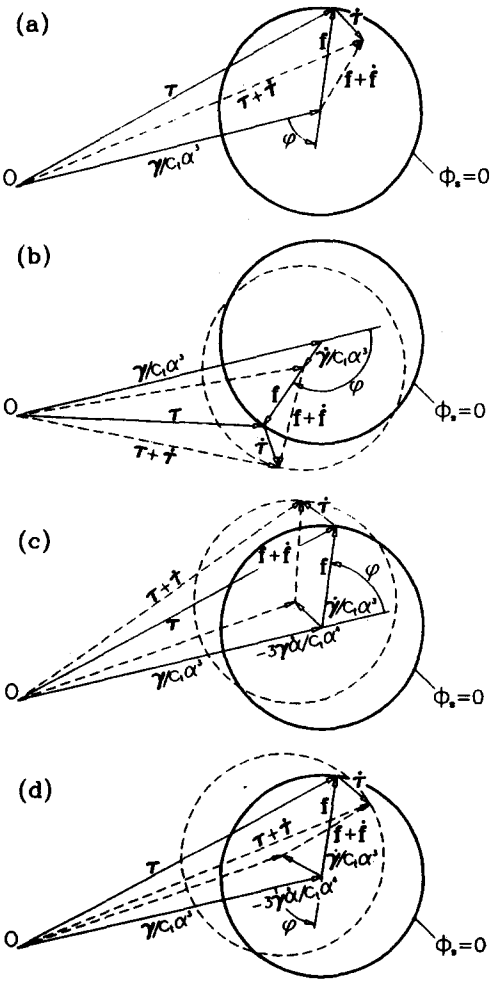

Fig. 1. Stress, friction and sliding rates and related motion of the no sliding domain in the plane of the tangential stresses ($\dot{\sigma} = 0$).

As in the above considerations relative to the open cracks, in the case of closed cracks the condition $\det \mathbf{A} = 0$ characterizes a limit state. Once this condition is attained, only stress rates inducing $\ell \leqslant 0$ are admissible to which two solutions correspond: the former involves the locking of the microcracks due to friction, the latter, which is unstable, is characterized by crack growth with sliding. The limit state is attained for values α and φ that satisfy the equation:

$$\mathscr{R}'(\alpha) - 2\mathscr{R}(\alpha)(1 - 3\sin^2\varphi)/\alpha = 0, \tag{33}$$

which is obtained from the equations $\dot{\Phi}_d^- = 0$ and $\det \mathbf{A} = 0$. Then, unlike the results for open cracks, it turns out that the value of the damage variable at the limit state depends on the loading path; however, for proportional loading paths, since $\varphi = 0$ (γ and $\mathbf{f}$ are parallel), eqns (33) and (23) coincide. From an analysis of eqn (33) it results that the minimum value for the solutions is α_c (corresponding to $\varphi = 0$); for growing values of the angle φ the value of the solution of eqn (33) increases, until a limit value φ^* is reached (depending on the $\mathscr{R}$ curve) beyond which no limit state can occur.

Finally for $\det \mathbf{A} < 0$ stress rates inducing $\ell > 0$ are not admissible; two different solutions may be obtained for $\ell < 0$. The former [see eqn (32g)] involves the locking of the microcracks and may be represented in Fig. 1(a); the latter [see eqn (32h) and Fig. 1(d)] corresponds to a slide with unstable crack growth.

With reference to the proportional loading paths, the analysis of the evolution equations and of the limit state conditions allow us to obtain, in the half plane $(\sigma, |\tau|)$, the limiting resistance curve and the limiting sliding line which delimit respectively the admissible stress states and the states in which no sliding takes place (Fig. 2).

For open microcracks ($\sigma \geqslant 0$) the limiting resistance curve, obtained from $\mathscr{D}(\alpha_c) = 0$, is expressed as follows:

$$\sigma^2 + \rho|\tau|^2 = \frac{\mathscr{R}'(\alpha_c)}{3c_n\alpha_c} = \sigma_t^2, \tag{34}$$

where σ_t may be assumed as a material parameter that represents, as it will be shown in the next section, the tensile strength in the direction $\mathbf{n}$. For closed microcracks ($\sigma \leqslant 0$) the limiting resistance curve is obtained from $\det \mathbf{A}(\alpha_c) = 0$, being $\varphi = 0$ for proportional loading paths; by substituting eqn (8b), bearing in mind that $\mathbf{f} = -\mu\sigma\boldsymbol{\tau}/|\boldsymbol{\tau}|$, and through the definition of the parameter σ_t given in eqn (34) the limiting resistance curve becomes

$$|\tau| + \mu\sigma = \sigma_t/\sqrt{\rho} = \tau_1, \tag{35}$$

where τ_1 is the shearing strength in the plane for vanishing normal stress.

Finally the limiting sliding line

$$|\tau| + \mu\sigma = 0, \tag{36}$$

is parallel to the limiting resistance curve.

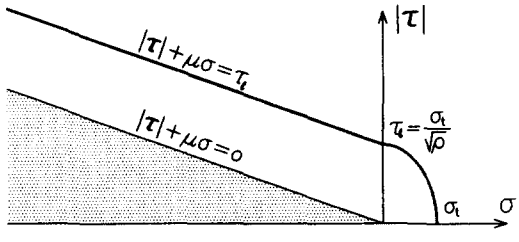

Fig. 2. Limiting resistance and sliding domains.

5. CONSTITUTIVE EQUATIONS AND FINITE STEP INTEGRATION ALGORITHM

The evolution equations formulated in the previous section for a subset of **n**-oriented cracks compel an incremental evaluation of the response of the microcracked solid. Through eqns (9), (10) and (14), after some manipulations, the macrostrain rate may be expressed as follows:

$$\dot{\mathbf{E}} = \mathbb{K}\dot{\mathbf{T}} + \sum^{\mathcal{N}^+} \alpha_i^2 \mathbb{H}_i[\alpha_i \dot{\mathbf{T}} + 3\dot{\alpha}_i \mathbf{T}] + \sum^{\mathcal{N}^-} \operatorname{sym}(\dot{\gamma}_i \otimes \mathbf{n}_i), \tag{37}$$

where $\mathcal{N}^+$ is the number of planes on which $\sigma_i \geqslant 0$, $\mathcal{N}^-$ is the number of planes on which $\sigma_i < 0$ and $\Phi_{si}^- = 0$ ($\mathcal{N}^+ + \mathcal{N}^- \leqslant \mathcal{N}$), the rates $\dot{\alpha}_i$ and $\dot{\gamma}_i$ are given by means of the evolution equations and the tensor $\mathbb{H}_i$ depends on the orientation $\mathbf{n}_i$ and on the compliances defined in eqn (7):

$$H_{i,\mathrm{rshk}} = (c_{ni} - c_{ti}) n_\mathrm{r} n_\mathrm{s} n_\mathrm{h} n_\mathrm{k} + \tfrac{1}{4} c_{ti} [\delta_{\mathrm{rh}} n_\mathrm{k} n_\mathrm{s} + \delta_{\mathrm{rk}} n_\mathrm{h} n_\mathrm{s} + \delta_{\mathrm{sh}} n_\mathrm{r} n_\mathrm{k} + \delta_{\mathrm{sk}} n_\mathrm{r} n_\mathrm{h}]. \tag{38}$$

Before facing the problem of integrating eqn (37) for finite load steps, it is worthwhile to note that in the initial phase of the loading process the model response is stable until the state for which the condition $\mathscr{D} = 0$ or $\det \mathbf{A} = 0$ is satisfied for some orientation. This state is a critical one for the model and the following stress rates are upper bounded ($\dot{\sigma} \leqslant 0$ or $\dot{t} \leqslant 0$); for proportional loading paths it identifies the upper bound for the multiplier of the applied stresses.

When the process is stress controlled, the states characterized by $\mathscr{D} \leqslant 0$ (or $\det \mathbf{A} \leqslant 0$) at some planes are unstable; in this case different subsequent paths are possible, related either to growing damage ($\dot{\alpha} > 0$) or to non-propagating microcracks ($\dot{\alpha} = 0$) at the critical crack planes, involving two different strain increments.

In strain controlled processes, once the critical state characterized by $\mathscr{D} \leqslant 0$ (or $\det \mathbf{A} \leqslant 0$) is attained, the model response may be stable or unstable. In fact, since the limit state at a single plane corresponds to a limit state for the model and the strain increments are defined as a sum of the strain in the elastic matrix and the contributions to strain related to the crack planes, the response of the present model may be unstable, exhibiting in this case the so-called snap back instability [see Bažant and Cedolin (1991)].

The integration of eqn (37) cannot be performed explicitly, except in very simple cases, and a numerical procedure must be employed, based on a loading path discretization in finite steps. With this aim, an increment $\Delta\mathbf{T}$ of the macrostress is considered in the load step, starting from the state defined by $\mathbf{T}$, $\mathbf{E}$ and α_i, γ_i ($i = 1, \mathcal{N}$); hence, in order to obtain the macrostrain increment $\Delta\mathbf{E}$, it is necessary to evaluate, in the load step and for each plane where one of the limit conditions (18), (24) or (26) is attained, the corresponding finite increment of the internal variables.

At a plane of the set $\mathcal{N}^+$, where the condition $\phi_{di}^+ = 0$ is attained, the damage increment $\Delta\alpha_i$, if allowed from (22), must satisfy the condition (18) at the end of the load step and thus can be obtained as the solution of the non-linear equation

$$\Phi_{di}^+(\sigma_i + \Delta\sigma_i, \tau_i + \Delta\tau_i, \alpha_i + \Delta\alpha_i) = 0. \tag{39}$$

Analogously, at a plane of the set $\mathcal{N}^-$, the increments $\Delta\gamma_i$ and $\Delta\alpha_i$ must satisfy the conditions (24) and (26) at the end of the load step. If the more general case is considered, which is characterized by $\phi_{si} = 0$ and $\phi_{di}^- = 0$ at the initial state, the increments $\Delta\gamma_i$ and $\Delta\alpha_i$, if allowed from (32), must satisfy simultaneously:

$$\Phi_{si}(\sigma_i + \Delta\sigma_i, \tau_i + \Delta\tau_i, \gamma_i + \Delta\gamma_i, \alpha_i + \Delta\alpha_i) = 0, \tag{40a}$$

$$\Phi_{di}^-(\gamma_i + \Delta\gamma_i, \alpha_i + \Delta\alpha_i) = 0. \tag{40b}$$

The non-linear equations may be solved through the following iterative procedure, starting with $\gamma_{i,0} = \gamma_i$ and $\alpha_{i,0} = \alpha_i$:

$$\begin{Bmatrix} \Delta\lambda_{i,k+1} \\ \Delta\alpha_{i,k+1} \end{Bmatrix} = \mathbf{A}^{-1}[\mathbf{v}_{i,k}, \gamma_{i,k}, \alpha_{i,k}] \begin{Bmatrix} \Phi_s(\sigma_i + \Delta\sigma_i, \tau_i + \Delta\tau_i, \gamma_{i,k}, \alpha_{i,k}) \\ \Phi_d(\gamma_{i,k}, \alpha_{i,k}) \end{Bmatrix}, \tag{41a}$$

$$\gamma_{i,k+1} = \gamma_{i,k} + \mathbf{v}_{i,k}\Delta\lambda_{i,k+1}, \tag{41b}$$

$$\alpha_{i,k+1} = \alpha_{i,k} + \Delta\alpha_{i,k+1}, \tag{41c}$$

in which the matrix $\mathbf{A}$ is that defined in (30), eqn (41b) represents a first order approximation of γ and

$$\mathbf{v}_{i,k}(\tau_i + \Delta\tau_i, \gamma_{i,k}, \alpha_{i,k}) = \frac{\tau_i + \Delta\tau_i - \gamma_{i,k}/c_{ti}\alpha_{i,k}^3}{|\tau_i + \Delta\tau_i - \gamma_{i,k}/c_{ti}\alpha_{i,k}^3|}. \tag{42}$$

The above procedure allows us to evaluate both the stable ($\det \mathbf{A} > 0$) and the unstable ($\det \mathbf{A} < 0$) solution.

Finally, once $\Delta\gamma_i$ and $\Delta\alpha_i$ are obtained for each orientation, the macrostrain increment $\Delta\mathbf{E}$ is evaluated through (37) by substituting finite increments for the infinitesimal ones.

6. RESULTS AND DISCUSSION

In the present section the response of microcracked, elastic, homogeneously stressed solids is analysed, which are characterized by two meaningful microcrack distributions: parallel cracks and randomly oriented cracks. The former distribution, which may be representative of layered materials, is the simpler one and the related results may be useful for a better understanding of the response of the latter one.

The crack growth resistance function $\mathscr{R}(\alpha)$ is chosen according to those proposed by Broek (1986) and Ouyang *et al.* (1990) with the aim of modeling the stable crack growth and the fracture process in quasi-brittle materials; it is defined as follows:

$$\mathscr{R}(\alpha) = \mathscr{r}(\alpha - 1)^{1/m}, \tag{43}$$

where the parameters $\mathscr{r}$ and m depend, through eqns (23) and (34), on the tensile strength σ_t, the critical ratio α_c and the extensional compliance c_n related to the orientation $\mathbf{n}$,

$$m = \frac{\alpha_c}{2(\alpha_c - 1)}, \tag{44a}$$

$$\mathscr{r} = \tfrac{3}{2}c_n\sigma_t^2[\alpha_c(\alpha_c - 1)^{1/\alpha_c - 1}]^2. \tag{44b}$$

Moreover, since $\mathscr{R}(1) = 0$, the $\mathscr{R}$ curve defined by (43) corresponds to the assumption of a progressive crack growth at each step of the loading process. Finally, from eqn (44a), it follows that the existence of limit states is allowed only if $m > 1/2$.

6.1. *Parallel microcracks*

A distribution of equioriented microcracks in an elastic isotropic matrix is considered, which corresponds to a transversely isotropic solid, representative of stratified materials such as schistose rocks and laminate composite materials undergoing damage in the interface between adjacent layers. The material response under uniaxial stress has been analysed for different crack orientations, defined by the angle β between the direction of the applied stress and that orthogonal to the crack planes.

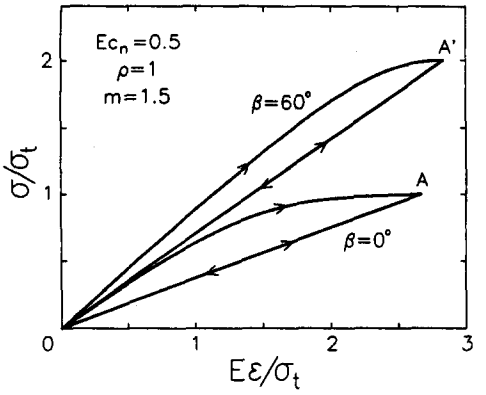

Fig. 3. Parallel microcracks: response to uniaxial tensile stress.

In Fig. 3 the stable response to tensile stress is shown, which exhibits both the typical stiffness degrading effect of the materials undergoing damage and the influence of crack orientation on the strength and the stiffness. The dependence of the tensile strength $\sigma_{t\beta}$, for which the limit condition $\mathcal{D} = 0$ is attained at the crack plane β-oriented, is obtained through eqn (34) and is expressed as follows:

$$\sigma_{t\beta} = \sigma_t \frac{1+tg^2\beta}{\sqrt{1+\rho tg^2\beta}}. \tag{45}$$

The overall modulus of normal elasticity E^*_β, related to stable β-oriented microcracks ($\alpha \cong 1$), is obtained through eqns (8) and (9) and is expressed as follows:

$$E^*_\beta = E^*_0 \frac{(1+Ec_n)(1+tg^2\beta)^2}{(1+tg^2\beta)^2+Ec_n(1+\rho tg^2\beta)}, \tag{46}$$

where E^*_0 corresponds to $\beta = 0$. The comparisons between the experimental results obtained by Nova and Zaninetti (1990) on schistose rocks under uniaxial tension, for varying inclinations of schistosity, and the theoretical results, from eqns (45) and (46), are shown in Fig. 4.

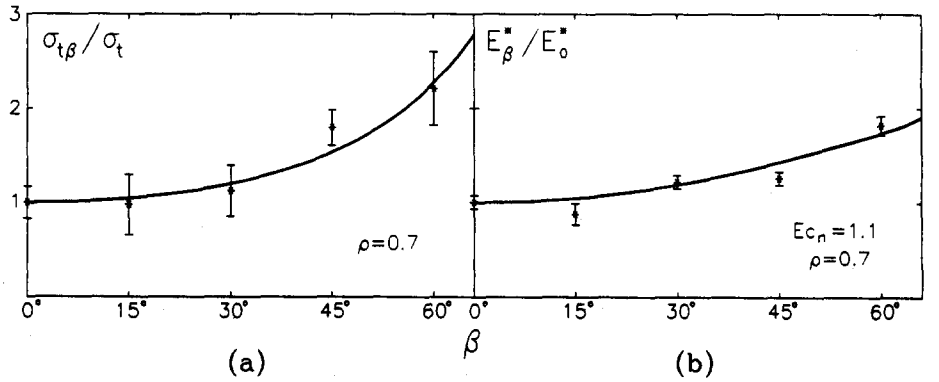

Fig. 4. Experimental and theoretical results on schistose rocks: (a) variation of the uniaxial tensile strength with crack orientation; (b) variation of the overall normal elastic modulus with crack orientation.

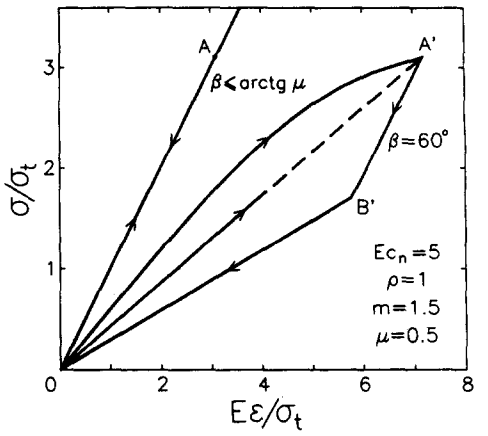

Fig. 5. Parallel microcracks: response to uniaxial compressive stress.

The graphs in Fig. 5 are related to the case of uniaxial compression and exhibit two qualitatively different responses: (a) for $\beta \leqslant \arctan \mu$ sliding is not allowed for and the response is that of the elastic matrix; (b) for $\beta > \arctan \mu$ sliding and damage occur at the loading phase OA′, while the unloading phase is characterized by a first no sliding phase A′B′ and a second one in which sliding occurs with no crack propagation until the stress and strain vanish. In the case (b) the dissipation is due to friction and damage in the step OA′ and to friction only in the step B′O.

The post-critical response, referred to the previously considered uniaxial loadings, may be stable or unstable in strain controlled processes according to the value of the material parameters: Ec_n, depending on the microcrack density, and m, which defines the shape of the toughness function. When low values of the parameter Ec_n, determining a small contribution of the anelastic strain, and when high values of the parameter m, representing a great fragility of microcracks, are considered, the model response exhibits snap-back instability.

6.2. *Randomly oriented microcracks*

Consider now the case in which no particular microcrack orientation can be detected in the material; in such a case a uniform distribution of microcrack orientations can be hypothesized (corresponding to the limiting case $\mathcal{N} \to \infty$), each orientation having an equal number of cracks of size a_0 at the initial stage. Let us consider a unit vector $\mathbf{n}$ and an infinitesimal solid angle $d\Omega$ as an orientation neighborhood of $\mathbf{n}$; in the unit volume the number of microcracks having a normal vector to the crack plane inside the orientation neighborhood of $\mathbf{n}$ is

$$dn = \frac{N}{2\pi} d\Omega, \tag{47}$$

where N is the number of all microcracks in a unit volume of the material. So eqn (9) can be rewritten in the form:

$$\mathbf{E} = \mathbb{K}\mathbf{T} + \int_{\Omega} [\varepsilon_i \mathbf{n}_i \otimes \mathbf{n}_i + \mathrm{sym}\,(\gamma_i \otimes \mathbf{n}_i)] \frac{d\Omega}{2\pi}, \tag{48}$$

where Ω is the half unit sphere representing all the orientations and ε and γ depend on the resolved stresses and the contact tractions at the crack plane of normal $\mathbf{n}$ through eqn (8), in which the compliances c_n and c_t have to be substituted respectively by the following terms:

$$h = \frac{N a_0^3}{E}\bar{g}(\nu), \quad k = \frac{N a_0^3}{E}\bar{\bar{g}}(\nu), \tag{49}$$

which are assumed to be material parameters ($k = \rho h$). This description implies isotropic stress–strain relations when damage does not take place and contact tractions are not effective.

In order to evaluate the response of the model to loading processes, the need arises to integrate a function related to the evolution equations defined on Ω; given the complexity of the evolution equations a numerical integration has to be performed which considers a finite number of orientations (to each one a weight w_i is associated), chosen in such a way as to approximate the material objectivity of the constitutive equations [see for example the integration scheme proposed by Bažant and Oh (1985)]. So, having in mind eqn (37), the finite increments of strain can be expressed as follows:

$$\Delta \mathbf{E} = \mathbb{K}\Delta T + \sum^{\mathcal{N}^+} \alpha_i^2 \mathbb{H}[\alpha_i \Delta T + 3\Delta\alpha_i \mathbf{T}]w_i + \sum^{\mathcal{N}^-} \text{sym}\,(\Delta\gamma_i \otimes \mathbf{n}_i)w_i, \tag{50}$$

where the compliance $\mathbb{H}$ is defined by (38), once the parameters c_n and c_t have been respectively substituted by h and k, and $\Delta\alpha_i$ and $\Delta\gamma_i$ are obtained by the algorithm proposed in the previous section.

First of all the stable response of the randomly oriented microcracked model to uniaxial tensile stresses is considered and is shown in Figs 6(a) and (b). The loading phase, up to the tensile strength σ_t, is characterized by a non-linearity due to the progressive anisotropic crack growth, while the unloading phase is linear and exhibits a reduced modulus and vanishing residual strains; further reloadings take place following this reduced modulus. The diagrams shown in Fig. 6(a) are obtained for some values of the dimensionless parameter Eh: for growing values of such a parameter, which is representative of the microcrack density, there is a corresponding compliance increase (for $Eh = 0$ no crack is present). In Fig. 6(b) the influence of the parameter m is shown, which rules the entity of the damage at the limit state [see eqn (44a)]; in the limit case $m \to \infty$, in which no crack grows, a linear response is obtained involving extensions and slides only.

The response to uniaxial compressive stresses is shown in Figs 7 and 8; the loading phase is characterized by a non-linear behavior due to the growth of the microcracks in which sliding takes place, which are those for which the angle between their orientation and the direction of the applied stress is greater than arctan μ. The compressive strength is given by

$$\sigma_c = 2/\sqrt{\rho}(\sqrt{1+\mu^2}+\mu)\sigma_t, \tag{51}$$

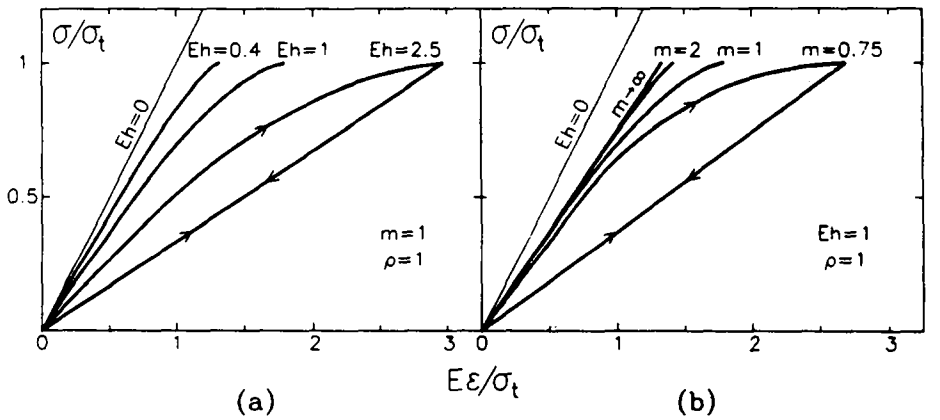

Fig. 6. Randomly oriented microcracks: response to tensile stress.

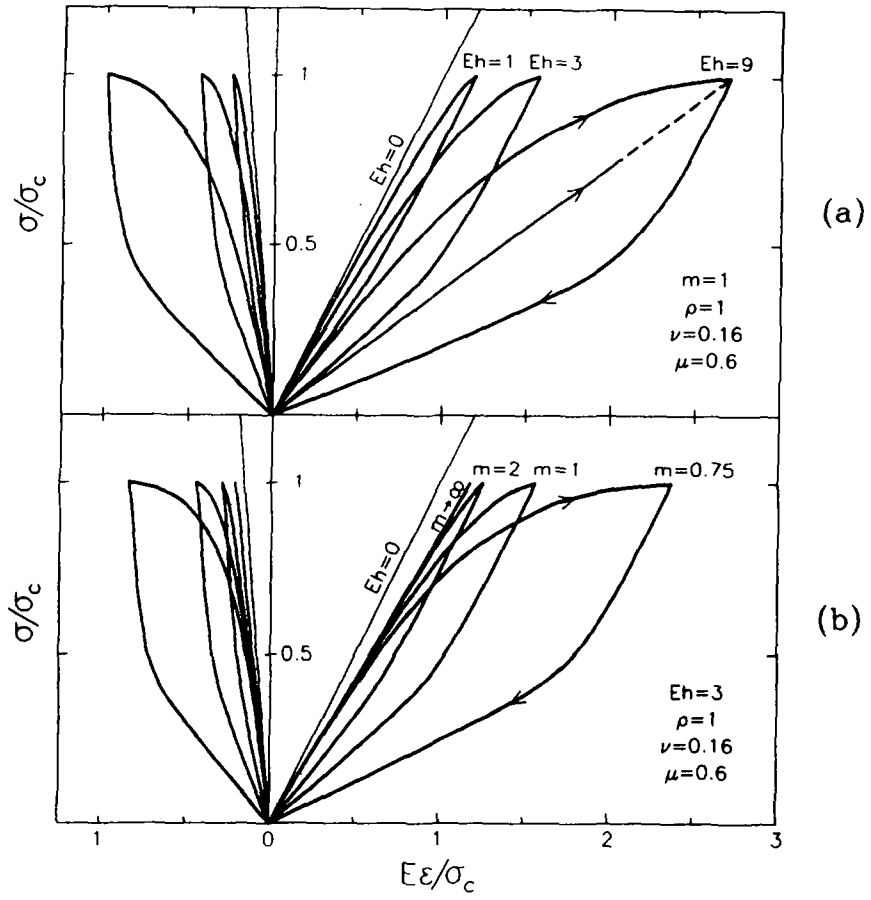

Fig. 7. Randomly oriented microcracks: influence of the parameters *Eh* and *m* on the response to compressive stress.

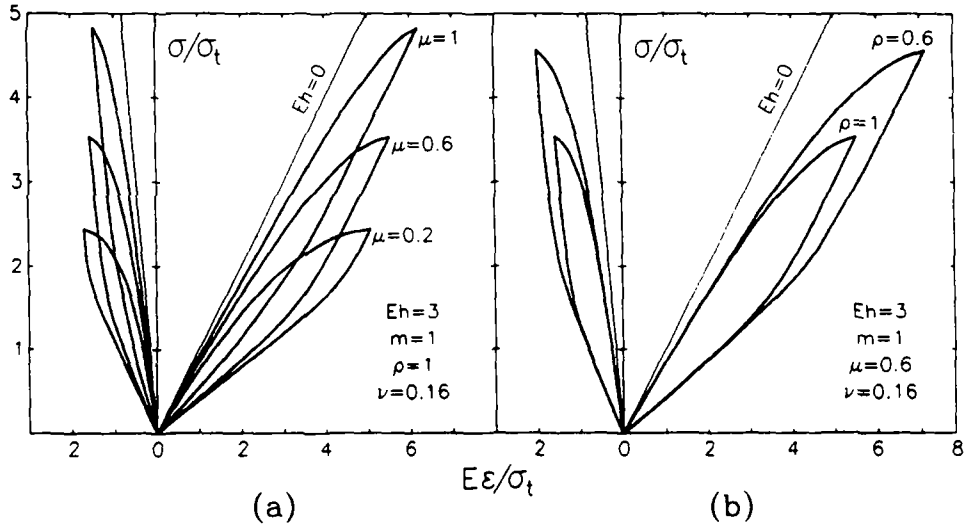

Fig. 8. Randomly oriented microcracks: influence of the parameters μ and ρ on the response to compressive stress.

which corresponds to the attainment of condition (35) on the cracks whose angle between their orientation and that of the applied stress is $\beta = [\pi - \arctan(1/\mu)]/2$. Analogously to the results of the parallel microcracked solid, the friction strongly affects the unloading response; the initial slope is that of the matrix ($Eh = 0$) and the following response is non-linear because of the progressive increase in the number of orientations in which slidings take place. In this phase no crack grows and no residual strain is present at the end of the unloading phase; furthermore the reloading response is linear, as shown by the dashed line in Fig. 7(a). The influence of the parameters Eh and m on the axial and the lateral strain is shown respectively in Figs 7(a) and (b).

In order to point out the friction effect on the compressive behavior of the model, stress–strain diagrams obtained for meaningful values of the friction coefficient are shown in Fig. 8(a); the diagrams show the influence both on the compressive strength [see eqn (51)] and on the cycle shape, with particular reference to the unloading curve. Figure 8(b) shows that the influence of the ratio ρ is effective only on the compressive strength and not on the cycle shape.

In the previous examples the tensile and compressive strength have been expressed; in general, when proportional loadings inducing triaxial stress states are considered, the limit resistance surface in the stress space can be obtained as the inner envelope of the limit resistance surfaces related to all the orientations, each of them obtained as the locus of the stress points satisfying the more restrictive of the limit conditions (34) and (35). If biaxial stress states are considered, the limit resistance domain for randomly oriented microcracks is that presented by Alpa (1984) and it is inscribed in those related to a finite number, $\mathcal{N}$, of orientations.

With the aim of showing the capabilities of the model in simulating the behavior of quasi-brittle materials, some experimental results on concrete obtained by Maekawa and Okamura (1983) are considered. In Fig. 9(a) the experimental results concerning cyclic compressive behavior, obtained for different values of the maximum compressive stress, are shown; the corresponding theoretical diagrams, shown in Fig. 9(b), are obtained by means of the following values of the model parameters: $Eh = 34.7$, $\rho = 0.3$, $\mu = 0.2$,

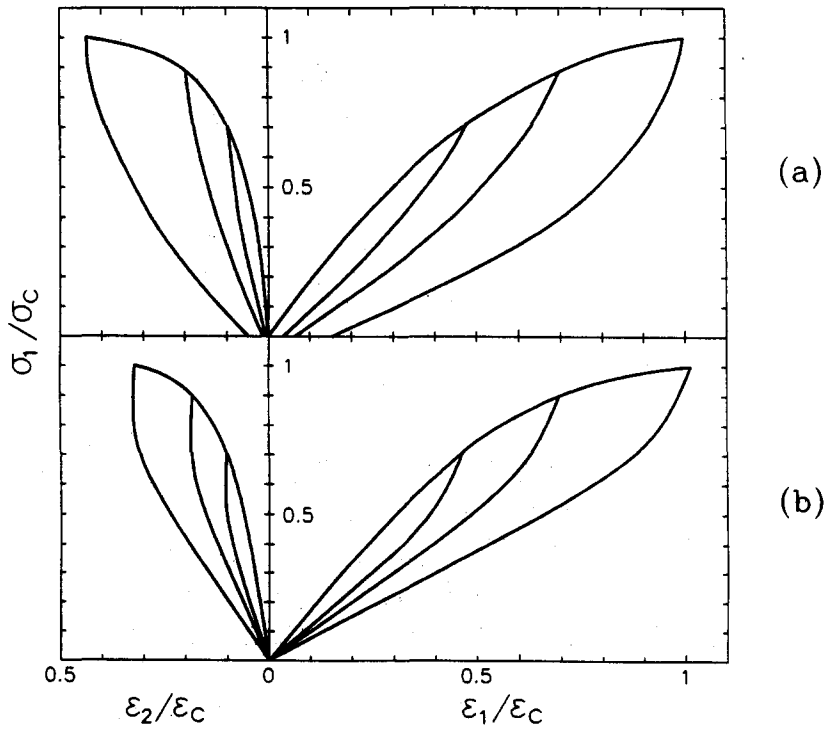

Fig. 9. Results obtained by cyclic compression on concrete: (a) experimental; (b) theoretical.

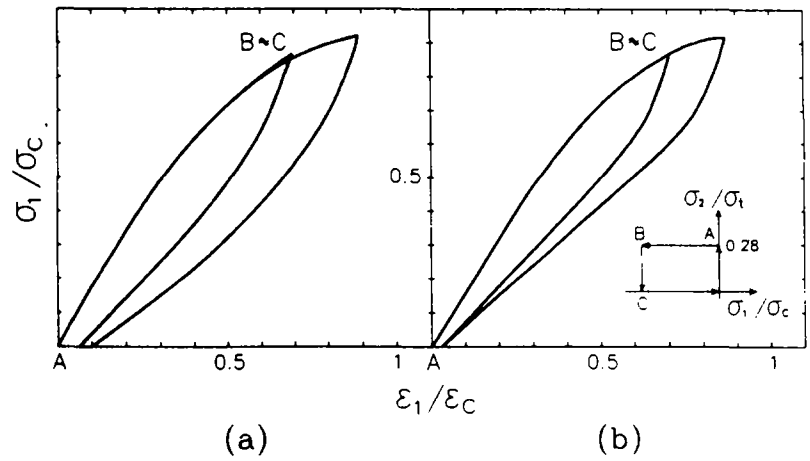

Fig. 10. Experimental and theoretical response of concrete under non-proportional loadings (first stress path).

$\nu = -0.17$, $m = 1.2$. It follows that a good agreement is obtained with reference to the first two cycles; in the cycle up to the compressive strength some differences may be observed in the lateral strain that is underestimated near rupture, since the model does not allow anelastic volumetric strain.

The capability of the proposed model in the case of non-proportional loadings is analysed by simulating experimental results from those obtained by Maekawa and Okamura on the concrete considered in the previous example and concerning biaxial stress states (the theoretical results have been obtained with the previously selected values of the model parameters). In the first loading path considered, the concrete is initially subjected to a tensile stress (up to $0.28\sigma_t$), then a lateral compressive stress is applied; the unloading phase is performed by unloading at first the tensile stress and then the compressive one. In Figs 10(a) and (b) the experimental and theoretical results are respectively shown. Vice versa in the second loading path a compressive stress is at first applied and then a lateral tensile stress; the experimental and theoretical results are shown respectively in Figs 11(a) and (b). In both the loading paths a good agreement appears between the experimental and the

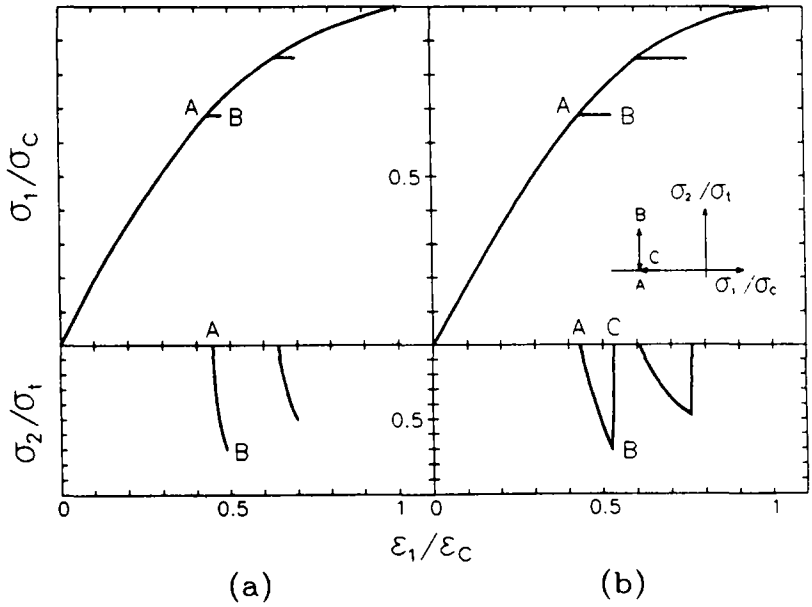

Fig. 11. Experimental and theoretical response of concrete under non-proportional loadings (second loading path).

theoretical results and, since the last ones have been obtained by assuming the material parameters deduced by the uniaxial compressive loading, the validity of the mechanical hypotheses at the base of the model is supported.

The last example considers a non-proportional loading path characterized by an initial relevant tensile stress (up to $0.75\sigma_t$), inducing a significant crack growth, followed by the application of lateral compressive stress. In Fig. 12 the response of the model is shown: in the initial phase of the compression AB a compaction effect is shown, which is due to the closure of previously opened microcracks, followed by the progressive stiffness degrading phase.

Let us consider now simple cases of the post-critical behavior of the model, supposing that the homogenization process, on which the formulation of the constitutive equations is based, is still admissible.

If uniaxial tensile stress is considered, the critical condition is attained on the plane normal to the applied stress. Afterwards only unloading steps are allowed to which there corresponds an unstable propagation of the critical microcracks and a linear response at the cracks of the other orientations, which are stable [see eqn (10)]. Since, according to the assumption of the continuum distribution of orientations, the subset of the critical microcracks has vanishing measure, their contribution to the strain is vanishing too; it follows that the strain depends linearly on the stress with a reduced modulus (in this case stable and unstable response cannot be distinguished). Similar results are obtained if uniaxial compressive stresses are considered; in this case, the limit condition is attained at the microcracks whose orientation is defined by an angle $\beta = [\pi - \arctan(1/\mu)]/2$ with respect to the direction of the applied stress (corresponding to a parallel of the half unit sphere of orientations). However, such a domain also has a vanishing measure so that the contribution to the strain in the unloading phase due to the unstable propagation of the critical microcracks is vanishing. A post-critical response of the model follows, which does not seem suitable for simulating the material behavior, since it corresponds to a limiting case of the snap-back instability with infinite brittleness [in the sense of Carpinteri (1989)]. This drawback comes from relating the crack growth criterion to the continuous distribution of the crack orientations in Ω, which is a material idealization suitable for the pre-critical response but not adequate for the post-peak phase. In fact, since the actual distribution of microcracks in the material is discrete both in amplitude and in orientation and the stress field is inhomogeneous, the critical state may be attained at nearly parallel microcracks.

An attempt may be considered which, by associating a finite measure $\Delta\Omega$ with the neighborhood of the orientation $\mathbf{n}$, assumes a finite number of orientations $\mathcal{N}$, according

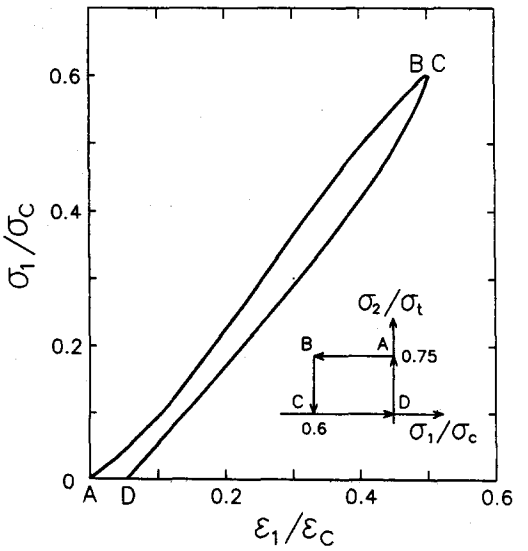

Fig. 12. Response to non-proportional loadings: compaction and stiffness degrading under compressive stress.

to the scheme in Section 2. In this hypothesis, when the limit condition is attained on the orientation $\mathbf{n}$, a finite number $n_i = N\Delta\Omega/2\pi$ of microcracks are at the limit state.

The choice of the $\mathcal{N}$ orientations must be such that the material symmetry group, which depends on the set of orientations, tends to the rotation group for $\mathcal{N} \to \infty$. For the response evaluation through eqn (50), the weight $w = \Delta\Omega/2\pi = 1/\mathcal{N}$ has to be associated with each subset and furthermore the number of subsets must be high enough for the resistance strength to come out markedly invariant with the choice of $\mathcal{N}$. However this condition does not seem to be restrictive; for example, if uniaxial tensile stress is considered, an appreciable divergence between the critical crack orientation and the stress direction has little effect on the tensile strength, as it may be observed from Fig. 4(a). It has been verified that such an approach, with reference to the stable response, leads to acceptable results provided that a number $\mathcal{N} > 30$ is assumed.

The sets of orientations satisfying the above-mentioned requirements correspond to the solutions of the problem of the regular tessellation of the unit hemisphere, which exist only for discrete values of $\mathcal{N}$; approximate solutions may be obtained by considering semi-regular tessellations [see for reference Coxeter (1973) and Onat and Leckie (1988)]. If only axisymmetric stress states are considered, inducing axisymmetric distributions of the internal variables, proper sets of $\mathcal{M}$ orientations can be easily obtained located in a diametral half-plane of the half unit sphere containing the axis of symmetry. The first orientation is chosen parallel to this axis, while the others define equal arches [of measure $\pi/(2\mathcal{M}-1)$] on the half meridian; the weight w_i associated with a generic orientation is chosen proportional to the area of the related spherical segment. This scheme may be assumed equivalent to a set of orientations in the three-dimensional representation, whose number is $\mathcal{N} \simeq 8(2\mathcal{M}-1)^2/\pi^2$.

The response to uniaxial tensile stresses is shown in Fig. 13. Figure 13(a) confirms the independence of the stable response from the number of orientations $\mathcal{N}$ (with reference to the considered range of values) and points out the marked influence of such a parameter on the post-critical response. With reference to strain controlled processes a stable response is obtained for $\mathcal{N} \simeq 400$ ($\mathcal{M} = 12$), while for $\mathcal{N} \simeq 1600$ ($\mathcal{M} = 23$) and $\mathcal{N} \simeq 4000$ ($\mathcal{M} = 36$) the snap-back instability takes place. Figure 13(b) shows the influence of the parameter m, related to the toughness function $\mathcal{R}(\alpha)$: by increasing the parameter m the transition from stable to unstable response is obtained.

Finally the response to uniaxial compressive stresses for varying $\mathcal{N}$ and m is shown respectively in Figs 14(a) and (b). In this case the transition from stable to unstable response is attained for a value of $\mathcal{N}$ higher than that related to the case of applied tensile stresses; in fact, as shown in Fig. 14(a), the snap-back instability takes place for $\mathcal{N} \simeq 120{,}000$ ($\mathcal{M} = 193$).

This behavior can be explained by considering the slope of the tangent to the stress–strain diagrams at the inception of the unloading phase for the limiting case $\mathcal{N} \to \infty$,

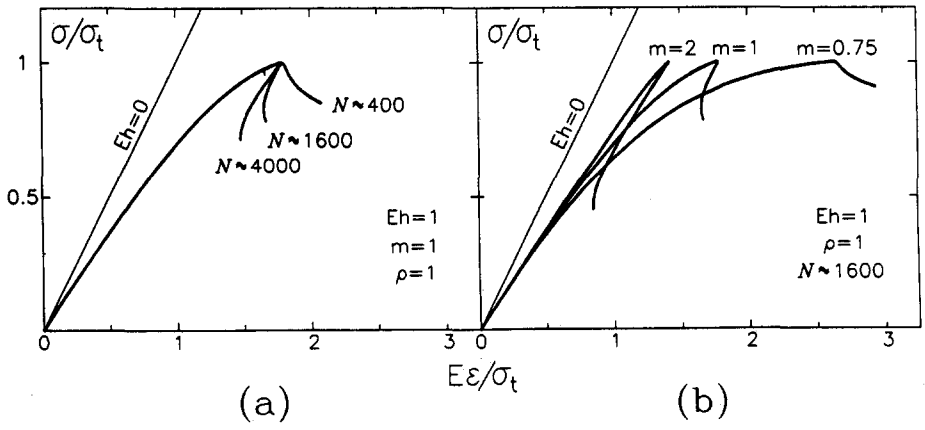

Fig. 13. Post-critical response to uniaxial tensile stress: (a) influence of the number of orientations $\mathcal{N}$; (b) influence of the parameter m.

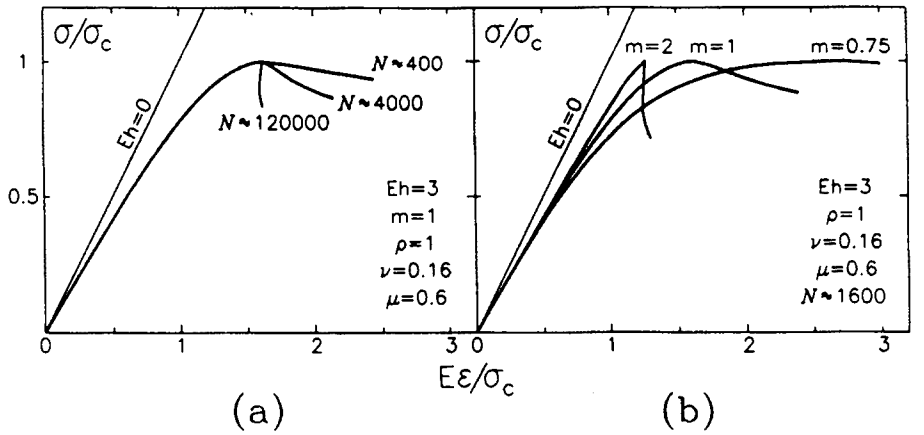

Fig. 14. Post-critical response to uniaxial compressive stress: (a) influence of the number of orientations $\mathcal{N}$; (b) influence of the parameter m.

when the measure of the critical orientations is vanishing. When compressive stresses are considered, the corresponding slope is that of the elastic matrix ($Eh = 0$), which is an upper bound, while if tensile stresses act, the slope is related to the secant modulus. As this difference in slope between the two stressing modes remains for finite $\mathcal{N}$, and the slope being increased for $\mathcal{N}$ diminishing, it follows that the change in sign of the slope, that is the transition from unstable to stable behavior, is first attained in compression for higher values of $\mathcal{N}$. Furthermore the influence of the number of orientations at the critical state must be considered; in fact when compressive stresses are applied, a greater number of critical orientations are effective, if compared with the case of applied tensile stresses, whose effect is to limit the tendency of snap-back instability.

7. CONCLUSIONS

Based on a vectorial representation of the damage, a microcrack model is developed which, by taking into account the unilateral friction contact between the microcrack faces, is able to describe the different behaviors of brittle and quasi-brittle materials under tensile or compressive stresses.

Comparisons between the theoretical and experimental results show the capability of the proposed model also when non-proportional stress paths are considered; several examples show some characteristics of the brittle materials' response such as anisotropic damage and loading path dependence.

Finally an interpretation of the different post-peak behavior of brittle and quasi-brittle materials under tensile and compressive stresses is given in the context of the present model. By introducing an appropriate parameter it is shown that the moderate brittleness observed when compressive stresses act may be interpreted as a consequence of the friction in the microcracks.

Acknowledgement—The present research was carried out with the financial support of the Ministero dell'Università e della Ricerca Scientifica (40%).

REFERENCES

Alpa, G. (1984). On a statistical approach to brittle rupture for multiaxial states of stress. *Engng Fract. Mech.* **19**, 881.

Bažant, Z. P. and Cedolin, L. (1991). *Stability of Structures*. Oxford University Press, New York.

Bažant, Z. P. and Oh, B. H. (1985). Microplane model for progressive fracture of concrete and rocks. *J. Engng Mech., ASCE* **111**, 559.

Broek, D. (1986). *Elementary Engineering Fracture Mechanics*. Martinus Nijhoff, Hingam, MA.

Carpinteri, A. (1989). Cusp catastrophe interpretation of fracture instability. *J. Mech. Phys. Solids* **37**, 567.

Coxeter, H. M. S. (1973). *Regular Polytopes*. Dover, New York.

Fanella, D. and Krajcinovic, D. (1988). A micromechanical model for concrete in compression. *Engng Fract. Mech.* **29,** 46.

Hashin, Z. (1988). The differential scheme and its applications to cracked materials. *J. Mech. Phys. Solids* **36,** 719.

Ju, J. W. (1991). On two-dimensional self-consistent micromechanical damage models for brittle solids. *Int. J. Solids Structures* **27,** 227.

Kachanov, M. L. (1982a). A microcrack model of rock inelasticity. Part I: Frictional sliding on microcracks. *Mech. Materials* **1,** 19.

Kachanov, M. L. (1982b). A microcrack model of rock inelasticity. Part II: Propagation of microcracks. *Mech. Mater.* **1,** 29.

Krajcinovic, D. (1989). Damage mechanics. *Mech. Materials* **8,** 117.

Krajcinovic, D. and Fanella, D. (1986). A micromechanical damage model for concrete. *Engng Fract. Mech.* **25,** 585.

Krajcinovic, D. and Sumarac, D. (1989). A mesomechanical model for brittle deformation processes: Part I. *J. Appl. Mech., ASME* **56,** 51.

Maekawa, K. and Okamura, H. (1983). The deformational behaviour and constitutive equation of concrete using the elasto-plastic and fracture model. *J. Fac. Engng Tokyo Univ.* Ser. B **37,** 253.

Nemat-Nasser, S. and Horii, H. (1990). Elastic solids with microdefects. In *Micromechanics and Inhomogeneity* (Edited by G. J. Weng, M. Taya and H. Abè), pp. 297–320. Springer, Berlin.

Nemat-Nasser, S. and Obata, M. (1988). A microcrack model of dilatancy in brittle materials. *J. Appl. Mech., ASME* **55,** 24.

Nova, R. and Zaninetti, A. (1990). An investigation into the tensile behaviour of a schistose rock. *Int. J. Rock Mech. Min. Sci.* **27,** 231–242.

Onat, E. T. and Leckie, F. A. (1988). Representation of mechanical behavior in the presence of changing internal structure. *J. Appl. Mech., ASME* **55,** 1.

Ouyang, C., Mobasher, B. and Shah, S. P. (1990). An $\mathscr{R}$-curve approach for fracture of quasi-brittle materials. *Engng Fract. Mech.* **37,** 901.

Sumarac, D. and Krajcinovic, D. (1987). A self-consistent model for microcracked-weakened solids. *Mech. Mater.* **6,** 39.

Sumarac, D. and Krajcinovic, D. (1989). A mesomechanical model for brittle deformation processes: Part II. *J. Appl. Mech., ASME* **56,** 57.